# PARTICLE FLUID HEAT TRANSFER IN SEMI-STRUCTURED ARRAYS USING RECONFIGURED CONSTANT TEMPERATURE ANEMOMETERS

**Kay A. BUIST[1], Bianca J.G.H. BACKX[1], Niels G. DEEN[1*] and J.A.M. (Hans) KUIPERS[1]**

[1] Multiphase reactors group, Department of Chemical Engineering & Chemistry,

Eindhoven University of Technology, P.O. box 513, 5600 MB Eindhoven, the Netherlands

*Corresponding author, E-mail address: N.G.Deen@tue.nl

## ABSTRACT

Many studies of particle-fluid heat transfer have been reported in literature. The work of Gunn (1972) is pioneering in this sense, as it provides a Nusselt correlation that covers all relevant flow conditions and particle packing fractions.

In Euler-Euler and Euler-Lagrange models the Gunn correlation is most often used to close the thermal energy balances. Recently, Direct Numerical Simulations (DNS) were conducted to confirm the applicability of these empirical correlations and extend upon them for the influence of, for instance, non-sphericity and wall effects. DNS techniques are usually validated with the aid of analytical solutions for limiting cases, like a single heated sphere in unbounded fluid. However especially at larger Reynolds numbers and in complicated geometries, it is difficult to make a quantitative comparison between simulations and experiments. The main reason for this is that experiments under these conditions are very difficult and time-consuming.

In this work, we present a novel experimental approach to study the effects of heat transfer for structured particle arrays. By employing an abacus-like structure we are able to control the local porosity. The measurement data of a Constant Temperature Anemometer (CTA) have been reinterpreted, so the anemometer can act as a heat transfer probe. The experimental setup allows us to vary the solids fraction from 0 to 0.6 with increments of 0.1 and Reynolds numbers ranging from 0 to 800.

## NOMENCLATURE

$A$    surface area, $m^2$
$L$    wire length, m
$Nu$ Nusselt number, -
$P$    Pressure, Pa
$Pr$ Prandtl number, -
$Q$    Heat flux, $J/(m^2\,s)$
$R$    Resistance, Ohm
$Ra$ Rayleigh number, -
$Re$ Reynolds number, -
$T$    Temperature, K
$V$    Voltage, V

$d$    particle diameter, m
$f$    momentum source term, $N/m^3$
$h$    heat transfer coefficient, $W/(m^2\,K)$
$k$    conductivity, $W/(m\cdot K)$
$q$    heat source term, K/s
$r$    radius, m

$t$    time, s
$u$    velocity, m/s

$\alpha$    Thermal diffusivity, $m^2/s$
$\varepsilon$    emissivity or porosity, -
$\sigma$    Stefan Boltzmann constant, $kg\cdot s^{-3}\cdot K^{-4}$
$\rho$    density, $kg/m^3$
$\mu$    dynamic viscosity, $kg/(m\cdot s)$

## INTRODUCTION

Because of the favourable mass and heat transfer characteristics fluidized beds are frequently used for many industrial applications. Nevertheless in certain gas-solid processes, such as in gas phase polymerization the release of massive amounts of heat leads to the formation of hot spots and agglomeration should be avoided. Therefore, proper understanding of hydrodynamics and heat transfer is of major importance.

The heat exchange between particles and the fluid is especially important. The correlation of Gunn (1978) is currently the most widely used to estimate fluid-particle heat transfer coefficients. Recently the development of direct numerical simulations have enabled detailed study of hydrodynamics and heat transfer in dense fluid-particle systems.

Correlations from these Direct Numerical Simulations are used as a basis for more coarse grained models as Discrete Particle Models and Two Fluid Models, following the multiscale modelling approach (van der Hoef et al., 2008). These coarse grained models need closures for the particle-fluid heat transfer.

DNS however is difficult to validate as often either the limiting cases or analytical solutions are the only available references (Tavasolli, et al., 2013). To properly compare the results of DNS with experiments very detailed control of the driving force and the local porosity is needed. Rexwinkel, et al. (1997) and Wakao & Kagei (1982) already discussed the difficulties of flow saturation on the analysis of the results. Works by, for instance, Happel & Epstein (1954), Yang, et al. (2012) and Mankad, et al. (1997) have tried to control the porosity, but these studies also show limitations in their analysis.

In this work we propose a novel experimental technique that is capable of controlling the driving force and the local porosity such that one to one comparison with DNS is possible. The technique is based on the use of a Constant Temperature Anemometer and an abacus like structure for the different packing fractions.

The results of this technique are directly compared to the correlations of Gunn (1978), Ranz (1952) and Ranz & Marshall (1952) as well as with simulation results of a single active particle in a structured array. The aforementioned empirical correlations are respectively given by:

$$Nu = \left(7 - 10\varepsilon + 5\varepsilon^2\right)\left(1 + 0.7\,\mathrm{Re}^{0.2}\,\mathrm{Pr}^{1/3}\right) + \left(1.33 - 2.4\varepsilon + 1.2\varepsilon^2\right)\left(\mathrm{Re}^{0.7}\,\mathrm{Pr}^{1/3}\right) \tag{1}$$

$$Nu = 2 + 0.6\,\mathrm{Re}^{0.5}\,\mathrm{Pr}^{1/3} \tag{2}$$

$$Nu = 2 + 1.8\,\mathrm{Re}^{0.5}\,\mathrm{Pr}^{1/3} \tag{3}$$

For the purpose of this work we interpolated the Ranz (1952) and Ranz & Marshall (1952) equations:

$$Nu = 2 + \left(-1.94\varepsilon + 2.54\right)\mathrm{Re}^{0.5}\,\mathrm{Pr}^{1/3} \tag{4}$$

## TECHNIQUES

### Constant temperature anemometer

Constant Temperature Anemometry (CTA) is a technique to study fluid flow. Often a thin wire or film is kept at a constant temperature by means of controlling the resistance in a Wheatstone bridge. The wire tends to cool down due to forced convection when subjected to a fluid flow.

The bridge will maintain a constant resistance by changing the top voltage. Via calibration the top voltage can be related to the fluid velocity. The top voltage is also a direct measure for the heat loss of the probe, following Joule heating. One of the older probes that is now out of use resembles in shape granular material that is currently under investigation in granular flow. In this work we will use a spherical CTA probe and relate the top voltage to the convective heat loss.
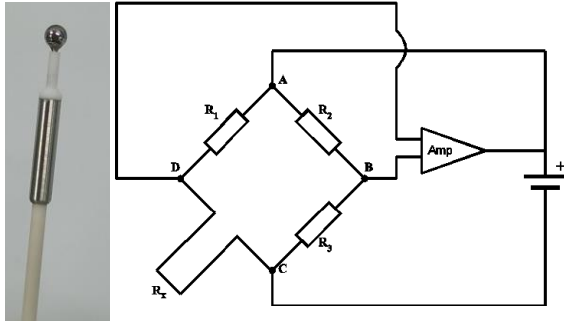


**Figure 1: The CTA-probe type 55R49 and the Wheatstone bridge with $R_X$ the probe resistance.**

Figure 1 shows the spherical CTA-probe which is one out of the four legs of the Wheatstone bridge. The probe is a omnidirectional CTA probe from Dantec type 55R49, 3.2 mm in diameter. $R_X$ denotes the probe resistance and $R_3$ is a resistance that can be set. The Wheatstone bridge is used to balance the ratio of $R_1$ over $R_2$ with the ratio of the bottom legs. The bridge is balanced by matching the top voltage with the needed heat loss, as such maintaining a constant probe resistance.

The probe resistance $R_P$ is temperature dependent and can be represented as follows:

$$R_p = R_{20} + \alpha_{20}R_{20}\left(T_p - T_{amb}\right) \tag{5}$$

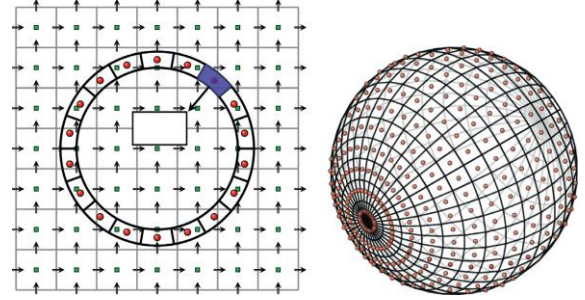The voltage over the probe is a function of the probe resistance $R_P$ and the top voltage:

$$V_p = V_{top}\left(\frac{R_p}{R_p + R_l + R_s + R_c + R_1}\right) \tag{6}$$

The corresponding Nusselt number is:

$$Nu = \frac{Q_p d_p}{A_p\left(T_p - T_{amb}\right)k_f} \tag{7}$$

with $Q_P$ following Joule heating as $Q_p = \dfrac{V_p^{\,2}}{R_p}$.

### Direct numerical simulation



**Figure 2: Illustration of the Direct Numerical Simulation method: Immersed Boundary method. (Tavassoli, et al. 2013)**

For the Direct Numerical Simulations (DNS) an Immersed Boundary (IB) method is used. The fluid dynamics is solved on a staggered Cartesian grid using the following equations:

$$\nabla \cdot \overline{u} = 0 \tag{8}$$

$$\rho_f \frac{\partial \overline{u}}{\partial t} + \rho_f \overline{u} \cdot \nabla \overline{u} = -\nabla P + \mu_f \nabla^2 \overline{u} + \overline{f} \tag{9}$$

$$\frac{\partial T}{\partial t} + \overline{u} \cdot \nabla T = \alpha_f \nabla^2 T + q \tag{10}$$

f and q in the above equations represent the momentum and heat source terms. These terms are used to respectively enforce the no-slip boundary condition for the flow and the Dirichlet boundary condition for the temperature. For more details the interested reader is referred to the work of Tavassoli, et al. (2013).

## SETUP

The experimental setup is schematically represented in Figure 3. The experimental setup consists of a flow chamber, where the flow is controlled by a 400 $L_n$/min mass flow controller. Moreover a pressure gauge by

Dwyer ranging from 0-1200 Pa and a thermocouple are connected to the setup to measure the ambient temperature, mounted inside the top section. The top section is exchangeable to account for the different porosity sections.

The top section consists of a square channel of 3-5 cm in width and 10 cm in height. 100 holes of 1 mm are drilled in two opposing side walls, through which strings of 0.12 mm are strung which hold the 3.2 mm copper beads in place. In total 5 rows are used and strung with beads, the middle row misses one particle to allow space for the probe.
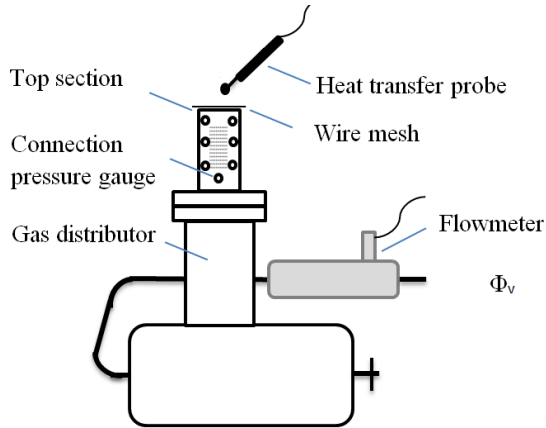


**Figure 3: Representation of the setup.**

The beads are 3.2 mm copper beads with a 0.9 mm centre hole by BeadFX. In total five top sections are made ranging from a porosity of 0.9 to 0.5, with 0.1 increments. For a porosity of 1 the probe is mounted in an empty top section and for a porosity of 0.4 the top section is completely filled as a randomly packed bed with 3-3.3 mm glass beads. Figure 4 shows an example of one of the top sections.
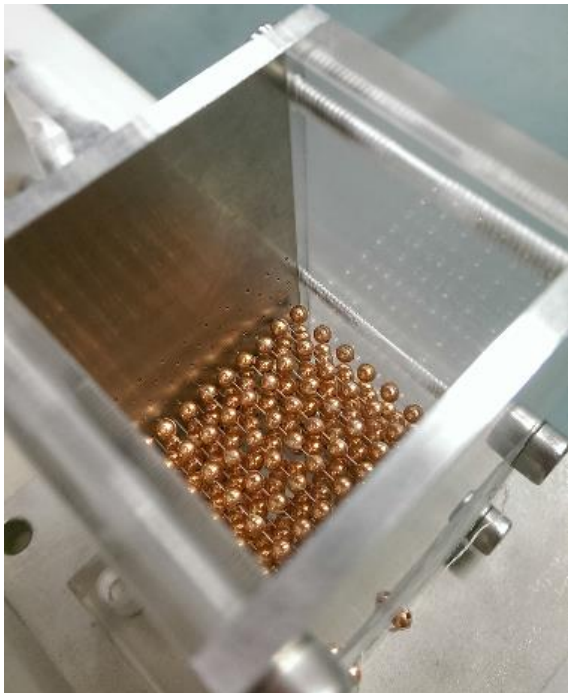


**Figure 4: One of the top sections with a porosity of 0.8.**

## RESULTS

As a first test the same limiting cases as typically used in the validation of the DNS are studied: a single sphere in unbounded flow and a packed bed. Direct Numerical Simulations have been run with varying Reynolds numbers ranging from 0 to 400. We found that the simulations for the single particle were grid independent with a grid spacing of 20 grids per particle diameter. For the packed bed system, simulations were first run at 20 grids per diameter to quickly generate a proper initial condition. The data was then interpolated to 40 grids per diameter and run again, saving a lot of computational time. In simulations, like in experiments, the particle in the centre has an elevated temperature of 60 °C. All the other particles are passive, which means that they are not actively heated. However, particles downstream of the active particle may slightly heat up though due to their interaction with the heated fluid.

The experiments for a single particle were varied from Reynolds 0 to 800. For the packed bed system the experiments could only be run up to Reynolds number 200. Above Reynolds numbers of 200 fluidization of the glass beads starts, which would have damaged the probe.
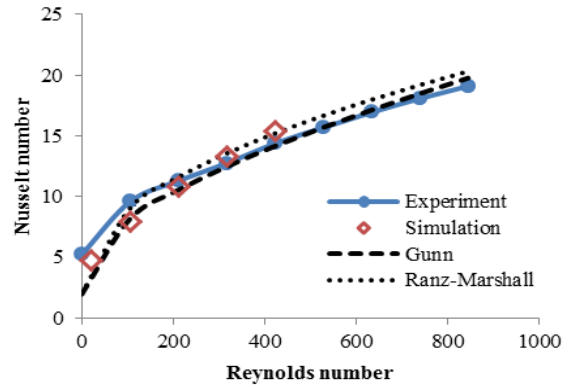


**Figure 5: Particle Nusselt number as a function of Reynolds number for a single particle in unbounded flow.**

Figure 5 shows the results of the single particle in unbounded flow. It can be seen that the experiments and simulations both follow the Gunn and Ranz-Marshall correlations very well with errors less than 20%. The only difference was found in the limit of Reynolds to zero, where other heat transfer mechanisms act in the experiments as well. These heat transfer mechanisms have been evaluated and the results are presented in Table 1.

**Table 1: Heat transfer mechanisms at Re=0.**

| Mechanism | Approximation | % of total at Re=0 |
|---|---|---|
| Total | Nu=5 | |
| Conduction | Nu=2 | 40 |
| Radiation | $Q = \varepsilon \sigma \Delta T^4 A_p$ | 10.4 |
| free convection | $Q = \dfrac{0.587 Ra^{0.25}}{\left(1 + \dfrac{0.469}{Pr^{9/16}}\right)^{4/9}}$ | 30.9 |
| wire conduction | $Q = 2\pi r_w{}^2 k_w \dfrac{T - T_{amb}}{L_w}$ | 10.55 |

| | | |
|---|---|---|
| wire convection | $Q = 4\pi r_w L_w h_w \left( T - T_{amb} \right)$ | 1.9 |

In total these heat transfer mechanisms account for 95% percent of the total heat loss found in our experiments. Especially the effect of free convection is important in understanding the differences between the experimental values and the empirical correlations, which assume the analytical solution of conduction at zero flow.

Figure 6 shows the results of the experiments and simulations for a packed bed situation. Simulations could be run for higher Reynolds numbers than the experiments, because the particles in the simulations are fixed and will not fluidize. Both simulations and experiments show a good comparison with the Gunn correlation. A slight underestimation is found for the experiments which might be partly result of the difficulty of stacking the beads in a closed packing form with the probe support at the top of the probe. This lowers the local solids fraction slightly and thus the heat transfer.
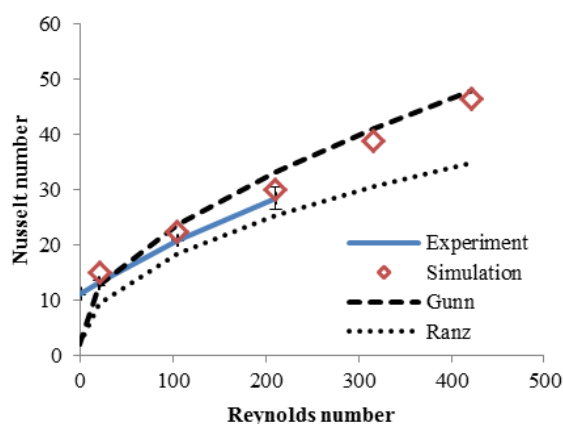


**Figure 6: Nusselt number as a function of Reynolds number for a packed bed, solids fraction 0.4.**

### Semi-structured beds

To be able to check the effects of porosity on the Nusselt number, semi-structured beds were made. By employing an abacus-like structure the local porosity could be controlled. Five semi-structured beds were made with solids fractions ranging from 10% to 50% with 10% increments. At the position of the probe one bead is left out to leave space for the probe.

Figure 7 shows the results of both the simulations as well as the experiments, compared to the Gunn and interpolated Ranz equations. In general it can be said that the results are in very good agreement. Also the parity plot of the experiments and simulations show a very reasonable agreement. In general the semi-structured experiments tend to be slightly higher than the simulations. The packed bed system on the other hand slightly underestimates the total heat loss. Both effects can be explained by the intruding effect of the probe support on the local porosity. In semi-structured beds the probe support adds to the total solids fraction thus lowering porosity and increasing local velocity and heat transfer. In a packed bed however the glass particles cannot nest tightly around the probe at the point where the support meets the probe thus increasing local porosity and lowering the total heat transfer rate.

## CONCLUSION

Constant Temperature Anemometers can be used as a heat transfer probe. In combination with a semi-structured bed formed with an abacus like structure the effects of porosity and Reynolds number on the Nusselt correlations can be measured.

First the CTA technique was validated with results of the Gunn and Ranz-Marshall equations as well as simulation results, of a single sphere in unbounded flow. Second the results were compared to a packed bed system with the Gunn and the Ranz equations. Both these limits show a good comparison of the CTA technique and the simulations. Lastly the probe was used in a semi-structured array. The results are in remarkable good agreement. This is the first time DNS could be validated over the full range of solid fractions and relevant Reynolds numbers.

Future studies have to be done to investigate the difference between DNS of a single active sphere in structured arrays as presented in this work and a fully active bed in random configurations as in the work of Tavassoli et al. (2013). Both the effects of active or passive surroundings and the effect of structured versus random packing should be studied.

Secondly the effect of polydispersity can be studied either in packed bed systems or with semi-structured arrays, in a similar way as shown in this work.

Third a comprehensive study of the heat transfer in fluidized beds would give more insight in the use of the correct closure equations. For instance a combination of Particle Image Velocimetry (PIV) and Infrared imaging (IR) could give more insight in the heat fluxes (Patil et al. (2015a)). A way must be found to get near adiabatic operation of the setup of Patil et al. (2015b).

## REFERENCES

GUNN, D., 1978. Transfer of Heat or Mass to Particles in Fixed and Fluidised Beds. *Journal of Heat and Mass Transfer,* **24(4)**, 467-476.

HAPPEL, J. & EPSTEIN, N., 1954. Cubical Assemblages of uniform spheres. *Industrial and Engineering Chemistry,* **46(6)**, 1187-1194.

MANKAD, S., NIXON, K. & FRYER, P., 1997. Measurements of Particle-Liquid Heat Transfer in Systems of Varied Solids Fraction. *Journal of food engineering,* **31(1)**, 9-33.

PATIL, A., PETERS, E. & KUIPERS, J., 2015b. Comparison of CFD-DEM heat transfer simulations with infrared/visual measurements. *Chemical Engineering Journal,* **277**, 388-401.

PATIL, A. et al., 2015a. A study of heat transfer in fluidized beds using an integrated DIA/PIV/IR technique. *Chemical Engineering Journal,* **259**, 90-106.

RANZ, W., 1952. Friction and transfer coefficients for single particles and packed beds. *Chemical Engineering Progress,* **48(5)**, 247-253.

4

RANZ, W. & MARSHALL, W., 1952. Evaporation from drops. *Chemical Engineering Progress*, **48(3)**, 141-146.

REXWINKEL, G., HEESINK, A. & SWAAIJ, W. v., 1997. Mass transfer in packed beds at low Peclet numbers—wrong experiments or wrong interpretations?. *Chemical Engineering Science,* **52**, 3995-4003.

TAVASSOLI, H. et al., 2013. Direct numerical simulation of particulate flow with heat transfer. *International Journal of Multiphase Flow,* **57**, 29-37.

VAN DER HOEF, M., VAN SINT ANNALAND, M., DEEN, N. & KUIPERS, J., 2008. Numerical Simulation of Dense Gas-Solid Fluidized Beds: A Multiscale Modeling Strategy. *Annu. Rev. Fluid Mech,* **40**, 47-70.

WAKAO, N. & KAGEI, S., 1982. *Heat and mass transfer in packed beds.* Taylor & Francis.

YANG, J. et al., 2012. Experimental analysis of forced convetive heat transfer in novel structured packed beds of particles. *Chemical Engineering Science,* **71**, 126-137.
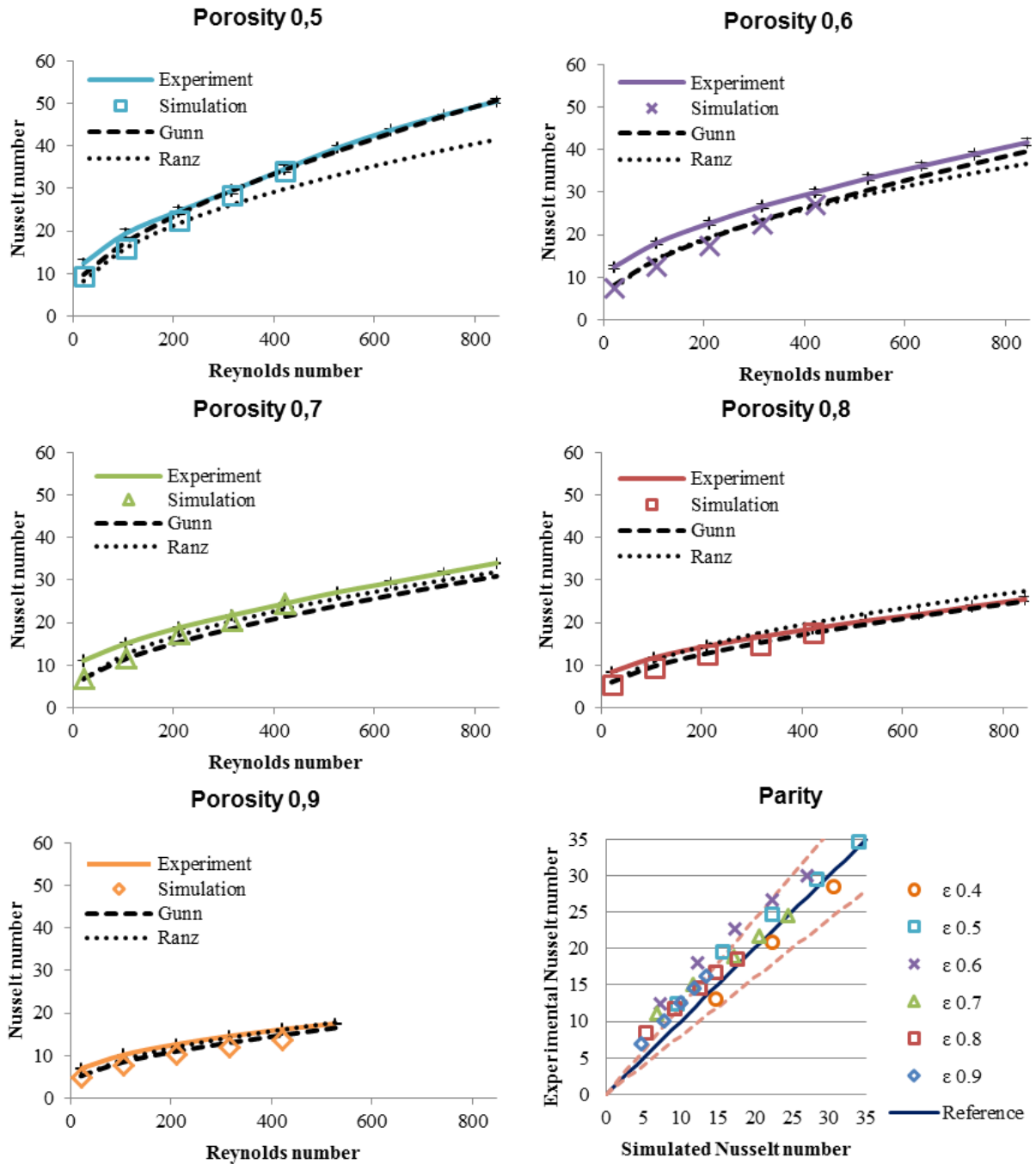
**Figure 7: Nusselt number vs. Reynolds number for varying void fractions. Bottom right parity plot of the experimental and simulation results with error margins of ±20%.**